CdS-Metal Contact at Higher Current Densities*

R. J. Stirn
Jet Propulsion Laboratory, Pasadena, California 91103

K. W. Böer and G. A. Dussel†
Department of Physics, University of Delaware, Newark, Delaware 19711
(Received 9 June 1971)

The current density as a function of applied voltage, optical excitation, and temperature in photoconducting CdS crystals with different non-Ohmic contacts (Au, Ag, Cu, Pt, Ni, and Sn) and the transient behavior of this current after switching-on of the applied voltage is investigated. High-field domains adjacent to these contacts are used as tools to measure the fields near the contacts. These domains are analyzed for different light intensities and temperatures. It is concluded from the experimental results that the observed high current density is caused by tunneling through the barrier and that in a slab of about 600-Å thickness at the cathode, the field must increase by about one order of magnitude from the field in the high-field domain. The space charge necessary for this must be stored in levels inaccessible for detection with conventional methods. It is proposed that in CdS about 10^{18}-cm^{-3} levels caused by native defects at about 0.8 eV below the conduction band are responsible for this space charge. These levels are probably also responsible for the fact that CdS is never observed to be *p* type under equilibrium doping conditions.

I. INTRODUCTION

The blocking properties of metal-semiconductor contacts are caused by a potential barrier in the interface region which is created by a mismatch between the work functions of the metal and the semiconductor. Some of the effects contributing to the work function depend on the state of the surface, as, e.g., the dipole contribution and the surface states. The latter may be different depending on whether the crystal is isolated or in intimate contact with another crystal. Hence, there are cases where barriers may show no correlation to the work function of the metal, i.e., Si, where it is believed that a high density of surface states pins the Fermi level at the surface, and cases where there is a strong correlation between them (this seems to be the case of CdS).

For crystals of low resistivity, the barrier height can be obtained by several methods in the limit of zero applied voltage (and therefore zero current); the most important are the study of the current-voltage characteristic, the voltage dependence of the capacitance, and the photoresponse. For crystals of high resistivity the bulk resistance may mask the influence of the contact region at low applied voltages. Photoconductors are in this category. However, the barrier still influences the current behavior. Under typical conditions the current in a photoconductor under reverse bias is of the order of 10% that under forward bias. The barrier acts as a *partial* limiter of the current, and forces a redistribution of the electric field in the interior of the crystal. Several mechanisms have been proposed by which electrons can overcome the barrier: thermionic emission, extraction of minority carriers, and tunneling through the barrier (also thermally assisted tunneling, or thermionic-field emission). At high applied voltages tunneling must predominate.

However, using the high-field-domain analysis, recent investigations[1] show that even at high applied voltages the electric field in the vicinity of the cathode is of the order of 50 kV/cm. In order to reach field values appropriate for tunneling close to the cathode a high density of space charge is required. In the observed absence of the necessary high density of states above the dark Fermi-level in CdS, it was concluded[1] that the barrier is lowered and that thermionic emission dominates.

The results presented in this paper extend the previous investigation, and make such barrier lowering improbable. Rather, it is concluded that tunneling (probably the multiple-step tunneling proposed by Parker and Mead[2]) must be the active mechanism, and a sufficient density of states to store the required positive space charge close to the cathode must be assumed at or below the dark Fermi level in CdS.

The main purpose of this and the following paper[3] is to show that a slab exists close to the cathode in photoconducting CdS in which the ordinary transport equation does not hold. This slab can be divided into two sections: a barrier section through which tunneling occurs, and an adjacent section which is defined by thermalization of the carrier momentum after tunneling. The carrier density and field at the end of the slab away from the contact determines the boundary conditions for the Poisson and transport equations in the remaining bulk.

II. GENERAL REMARKS

In the present paper we are mainly interested in the mechanisms by which the contact allows a steady flow of current as required by the bulk of the crystal under the application of an external voltage.

The contact region is shown in Fig. 1. It is characterized by several parameters. The height of the barrier is ψ_0 in the absence of external fields and ψ in the presence of external fields. The difference is given by

$$\psi_0 - \psi = \Delta V = (eF/4\pi\epsilon_0\epsilon_\infty)^{1/2} , \qquad (1)$$

where F is the electric field in the barrier region (assumed to be constant), ϵ_0 the permittivity of free space, and ϵ_∞ the optical dielectric constant.

The position of the top of the barrier is x_b, which, taking account of the image force, is given by

$$x_b = \left(\frac{e}{16\pi\epsilon_0\epsilon_\infty F} \right)^{1/2} . \qquad (2)$$

For fields of order or above 10^5 V/cm, x_b becomes smaller than the mean free path. This sets a limit to the validity of a statistical approach in the barrier region. The space-charge region is assumed to extend to a distance x_s. A parameter of importance in the present discussion is x_0, which we define as the point beyond which ($x > x_0$) the usual transport and Poisson equations are valid; this distance x_0 will be discussed in more detail and its value will be estimated in the second paper.[3]

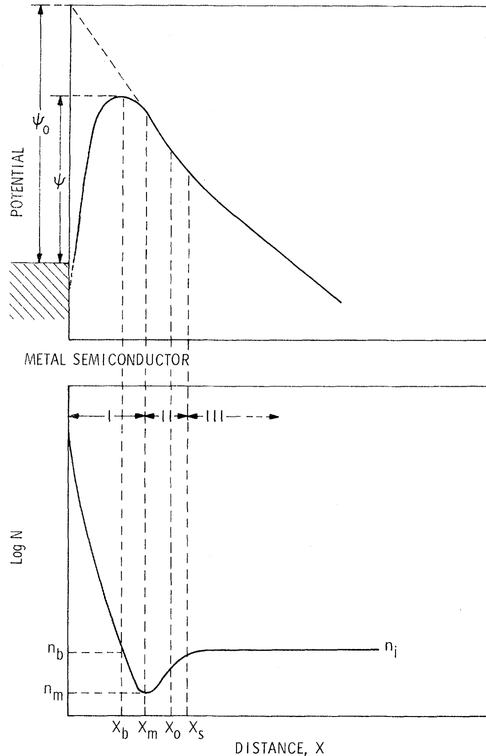

FIG. 1. Potential energy and carrier distribution vs distance from the interface, with applied field, showing the image force region (I) and the space-charge region (II).

For clarity of the presentation, we will review briefly the main characteristics of the current mechanisms.

a. Photoemission from the cathode. In CdS this is only important if there is little bulk excitation. It is successfully used for the determination of barrier heights.

b. Thermionic emission. This is the flow of electrons which are thermally excited over the barrier from the metal. The upper limit of the current obtainable in this model is given by

$$j_s = \frac{ev_{\text{th}}}{6\pi} n_b \simeq 10^{-12} n_b \text{ A/cm}^2 , \qquad (3)$$

where

$$n_b = N_c e^{-\psi/kT} . \qquad (4)$$

is the density of electrons at the top of the barrier, N_c is the effective density of states, and v_{th} is the thermal velocity. At sufficiently low applied voltages, when $j < j_s$, the current can be obtained from

$$j = eD \left(\frac{dn}{dx} \right)_{x_b} , \qquad (5)$$

where D is the diffusion constant, since the electric field vanishes at the top of the barrier. In the case of the Au–CdS contact, we have $\psi_0 = 0.8$ eV, and at room temperatures we find $j_s \simeq 10^{-8}$ A/cm^{-2}, while at 150 °K, $j_s \simeq 10^{-23}$ A/cm^{-2}.

c. Minority-carrier extraction. Minority carriers generated by light in the space-charge region can be swept out into the metal by the field. There are as many majority carriers contributing to the current as the amount of minority carriers swept out in unit time. Otherwise, the crystal would become charged. Therefore, this mechanism requires the gain factor to be much smaller than one and at best to be given by (assuming that the field in the space charge region is large enough to sweep out the generated holes)

$$G = \frac{j}{eaL} = \frac{x_s}{L} , \qquad (6)$$

where L is the length of the crystal and a is the volume excitation.

d. Tunneling of electrons. In order that tunneling currents can compete with the other mechanisms, high fields are required in the barrier region. In cases in which there is an intermediate state (Coulomb-attractive potential) due to a high density of imperfections, the fields required are of the order of 3×10^5 V/cm (multiple-step tunneling). For thermally assisted tunneling or direct tunneling

(i. e., from the Fermi level in the metal), fields somewhat higher (of the order of 10^6 V/cm) are required for the high current densities observed in the experiments reported here.

Obviously, from such simplified models one can learn little about the actual physics of the contact to high resistivity semiconductors and it is impossible to attribute the observed behavior to surface states, tunneling, or mere barrier lowering without a more detailed analysis of the actual potential distribution near x_b and the current transport in this region.

Unfortunately, experimental information about the barrier region was rather limited and almost exclusively of indirect nature. The most valuable information was obtained from current-voltage characteristics at low applied voltages (< 1 V), barrier capacity measurements, and studies of the spectral distribution of the photoresponse. Only very recently a method using high-field domains was developed to determine unambiguously the field near the contact,[4,5] at the position x_0 (of the order of a few hundred Å) as we will show in the following theoretical paper.[3] We will apply the high-field-domain analysis to aid our investigation of the near-contact region and discuss it in more detail in the following section.

We will also measure the time dependence of the current shortly after the voltage is applied and before a high-field domain is completed, since the formation of a thin layer of high space-charge density is necessary to allow for the observed current. The build-up of such a space-charge layer to accommodate the changing demand of current flux by changing the space-charge distribution in times well accessible to observation (10^{-6}–10^1 sec) is highly instructuve for the understanding of the barrier layer.

We have therefore continued our investigation in these two fields and will report the results in the following sections. In the following paper[3] we will analyze the results theoretically, using a more detailed model of the space-charge region.

III. HIGH-FIELD DOMAIN ANALYSIS

Before we enter the description of the experiments, it is helpful to analyze stationary high-field domains in more detail[4,6,7] and to point out which information is helpful for the understanding of blocking contacts. We will use the Poisson and simple transport equation

$$\frac{dF}{dx} = \frac{e}{\epsilon\epsilon_0}\rho(F,n) , \tag{7}$$

$$j = en\mu F - \mu kT\frac{dn}{dx} , \tag{8}$$

as a basis for the discussion; hence, we are restricted to a region $x > x_0$ in which this system of equations describes a valid model.

Equations (7) and (8) represent an autonomous system of differential equations which can be rewritten as

$$\frac{dF}{dx} = \frac{e}{\epsilon\epsilon_0}(n + n_t - p - p_t) , \tag{9}$$

$$\frac{dn}{dx} = \frac{1}{\mu kT}(en\mu F - j) , \tag{10}$$

with $n_t(p_t)$ the sum of all negatively (positively) charged states (traps). (The signs of F and j are chosen so that they are in the direction of electron flow.) The quantities n, n_t, p, and p_t will depend on the field at higher field strength. The solutions of Eqs. 9 and 10 are best discussed graphically in the field of direction[4,5] in an n, F plane. This discussion is facilitated by introduction of two auxiliary functions $n_1(F)$, the quasineutrality curve for which $dF/dx \equiv 0$, hence $n_1 = p + p_t - n_t$, and $n_2(F)$, the drift current curve for which $dn/dx \equiv 0$, hence $n_2 = j/e\mu F$. These curves are shown in Fig. 2 for a typical case. The decrease of $n_1(F)$ at medium fields is caused by field quenching, the adjacent steep rise probably caused by field emission from traps. The horizontal part in $n_2(F)$ is caused by a field-dependent mobility[8] $\mu(F) \propto 1/F$.

Below $n_1(F)$ and $n_2(F)$, n and F decrease with increasing x (measured from cathode to anode). Therefore, the direction of a solution of Eq. (10) through any point in this sector must lie in the third quadrant ($180° < \phi < 270°$), and is symbolized by a small arrow pointing left down. Similarly, the directions in the other sectors of Fig. 2 are symbolized by their respective arrows.

In this model the solution curve starts at x_0 and can easily be constructed for $x > x_0$ if $n(x_0)$ and $F(x_0)$ are given. However, when a high-field domain ap-

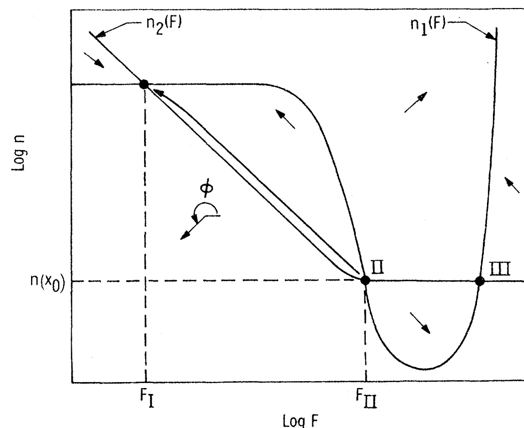

FIG. 2. Symbolized field of direction (indicated by small arrows) with charge neutrality curve $n_1(F)$ and drift current curve $n_2(F)$, and a typical solution (heavy arrow) in the cathode-adjacent high-field domain region.

pears, essentially (with little error) only one boundary condition is necessary to determine the solution in Fig. 2 since a domain solution extends from the close neighborhood of one singular point [intersection of curves $n_1(F)$ and $n_2(F)$] to the close neighborhood of another singular point.[4,7] Such a solution is shown in Fig. 2 by the arrow starting at $n(x_0)$. It extends between singular points II and I (cathode near II) with a field F_{II} in the high-field domain and field F_I in the adjacent low-field region. The transition between these two regions occurs within a length of the order of a few Debye lengths and hence is rather abrupt in the investigated crystals, which are long compared to the Debye length (see below).

The field in the high-field domain can be easily determined by measuring the domain widths for two different applied voltages[4,7] and usually lies in the 50–100 kV/cm range. (In the domain range the current does not change with the applied voltage V; hence F_I and F_{II} are constant and only the domain width increases with V).

It is important to know for our further discussion on contact properties whether the solution starts near a singular point II as shown in Fig. 2, or whether it starts at much higher fields and a high-field domain appears because the solution "squeezes" through a quasisingular region[7] II* as shown in Fig. 3. Since the current is lower in Fig. 3 than for the case pictured in Fig. 2, a simple method for checking which of the two cases is present is to apply additional infrared quenching to the crystal. In the case of Fig. 2, the current must decrease with sufficient infrared irradiation since F_{II} is not high enough to achieve complete quenching. In the case of Fig. 3, no further quenching can be induced with infrared since II* represents the fully quenched state and the current remains constant even with high-intensity quenching light.

As shown later in this paper, the case of Fig. 2 applies for the contacts used on CdS. Thus, one must conclude that the field for $x > x_0$ within the high-field domain is essentially equal to F_{II}. It cannot exceed F_{II} since the field of directions does not allow the solution to reach F_I from any point above F_{II}.

In the high-field domain the space-charge density is negligible, since F remains close to F_{II}. The space charge density must decrease to below 10^{12} cm^{-3} within the domain, since in the entire domain the field does not decrease within the experimental error (± 5%) below F_{II}, with the high-field domain possibly extending over the entire crystal[4,7] (at sufficiently high applied voltage). The decrease from $\rho = 10^{17}$ cm^{-3} at x_0 to below 10^{12} cm^{-3} must occur rather abruptly near x_0, for F not to decrease markedly below F_{II}.

The domain analysis, therefore, provides a reliable method to measure the field at x_0 for electrodes yielding boundary conditions resulting in cases pictured in Fig. 2. Any behavior for $x < x_0$ cannot be described by this analysis and this case is discussed in the second paper. However, it should be noted that the entire system tends to select a state with the lowest possible current density (minimum-entropy production principle[9]). The boundary condition $n(x_0)$, therefore, is unambiguously determined by the properties of the slab $x < x_0$, and yields a solution passing through the near vicinity of the singular point II if the case of Fig. 2 is experimentally observed.

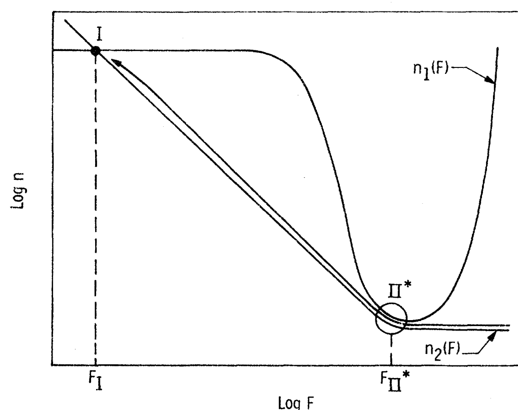

FIG. 3. Same as Fig. 2, but for a lower carrier concentration at the boundary so that a solution curve would start at a higher field than shown in Fig. 2.

IV. EXPERIMENTAL

CdS single-crystal platelets doped[4] with 50-ppm Al and 50-ppm Ag were used. The platelet was sawed with a wire saw perpendicular to the c axis into strips typically 0.4 mm wide. The strips were cleaved parallel to the c axis in a vacuum of about 10^{-7} torr while evaporating the metal onto the freshly cleaved surface. For cleaving, the lower part of a platelet strip was imbedded in wax and a moving blade was made to strike the protruding edge of the strip. The second electrode on the opposite surface was evaporated after the wax was dissolved and after a small piece of the lower part of the platelet strip was cleaved-off in air ambient.

Several of the crystals were cleaved on both ends outside the vacuum system and immediately thereafter mounted for evaporation of the metal electrodes, avoiding any physical contact to the freshly cleaved surface before evaporation.

The crystals of typical dimensions $0.1 \times 0.4 \times 0.5$ (electrode distance) mm^3 were then imbedded in epoxy and positioned between two glass cover plates as described earlier.[1] For the investigation of high-field domains, the crystals were illuminated with band-edge light and the Franz-Keldysh effect

was used to observe the domain[1] and to measure its width with the aid of an ocular micrometer.[10] For purposes of changing the crystal temperature the crystal was positioned on a cooling finger in a glass container filled with dry N_2.

The current-voltage characteristic was measured using a regulated power supply damped with an external RC of about 10 sec and slowly changing the applied voltage while recording the voltage and current with an x-y recorder using a Keithly 417 $\mu\mu$-ammeter.

For measuring current transients after switching on the applied voltage, a set-up as shown in Fig. 4 was used. By carefully shielding the leads to the crystal, its effective capacity was reduced to to ~ 3 pF. Different parts of the transient characteristic were sequentially measured by exchanging the current-sensing resistor. Reproducibility and continuity were checked by considerable range overlapping. A mercury-wetted relay switch was used with proper contact conditions established within about 10^{-6} sec. Reproducible data unaffected by circuit time constants were obtained for times beyond 10 μsec after switching, with a 1-MΩ probe and a Tektronix 3A9 plug-in/564 storage oscilloscope.

V. EXPERIMENTAL RESULTS

No marked differences were detected in the electrical properties (as reported here) for CdS crystals cleaved in air or in vacuum.

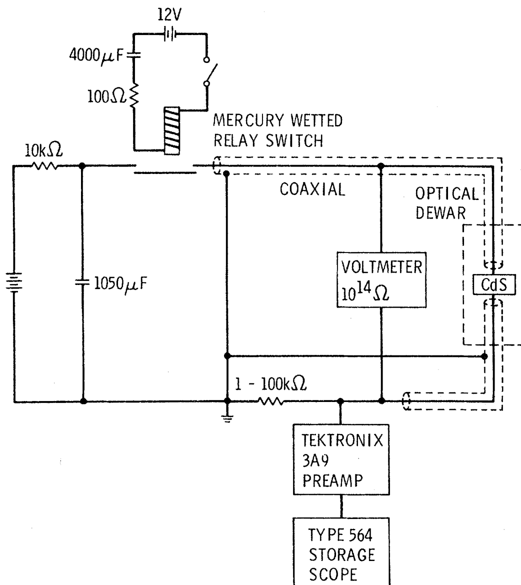

FIG. 4. Experimental arrangement for the measurement of current transients after switching on the applied voltage.

A. High-Field Domains and Stationary Currents

The electron density in the crystal bulk as a function of the actual external fields is an important parameter for a detailed analysis of the behavior near the contact. It has been measured using the method of high-field domains and a shadow as quasicathode[5] between Ohmic Ti/Al electrodes at the outer edges. This measurement was done with the crystal platelet before it was sawed and cleaved into the pieces which were finally used. For further detail of this measurement, we refer to an earlier publication.[5] The observed $n_1(F)$ curve is shown in Fig. 5. The measurements were done at 200 °K and with an optical excitation of 5×10^{16} photons/cm^3 sec. The steep decrease in $n_1(F)$ between 30 and 100 kV/cm is caused by field quenching.[6] Only in this range does $n_1(F)$ depend markedly on doping. At higher fields where the doping influence is less pronounced, the curve is extended (dashed part) using the results obtained from similar CdS crystals[7] with an extrapolated $1/F$ law for the mobility.[8]

The results reported here stem from small pieces cut from this crystal platelet. Hence, they all have about the same doping. The reported behavior is fairly well reproducible from crystal to crystal of the same platelet, but differs quantitatively somewhat for crystals cut from a different platelet (indicating the influence of slightly different doping).

Figure 6 shows the fields in the cathode-adjacent high-field domain as a function of optical-excitation density and temperature for a number of cathode metals. In all cases infrared quenching reduces the saturation current. Hence, F_{II} is determined by an actual intersection between $n_1(F)$ and $n_2(F)$ as shown in Fig. 2.

From Fig. 6 it is seen that the field in the high-field domain depends on the cathode metal, increases slightly with the intensity of optical excitation, and (neglecting a small maximum near 200 °K) decreases slightly with increasing temperature. In most cases it varies over a rather narrow range between 50 and 70 kV/cm and occasionally has extended as low as 35 kV/cm and as high as 125 kV/cm.

In Fig. 7 the measured current density is given as a function of the applied voltage (for voltages smaller than the critical voltage to cause high-field domains), and of the optical-excitation density and temperature (for applied voltages in the current saturation range). The current density depends on the cathode material and changes with applied voltage, optical excitation, and temperature, in the usual manner. It behaves similarly for the different cathode metals. The higher the electronegativity of the metal (with the exception of Pt), the smaller the current is at a given voltage.

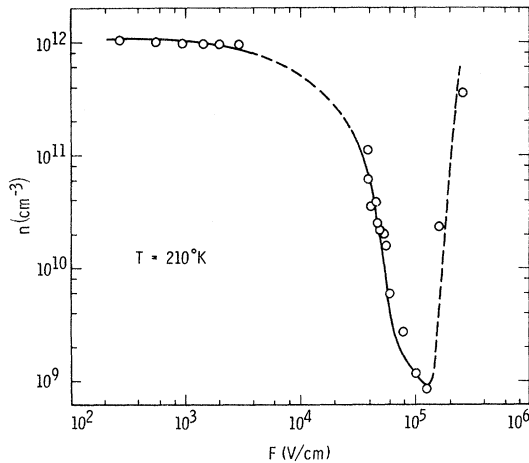

FIG. 5. Measured electron density in the bulk as a function of applied field at 200 °K and at an optical excitation of 5×10^{16} photons/cm^3 sec^1.

B. Nonstationary Measurements

Typical kinetic behavior when biasing in the reverse direction is very similar for all "blocking" contacts, and is shown in Figs. 8(a) and 8(b) for two different temperatures and voltages with optical-excitation density as a variable. After switching on the voltage (in reverse direction), the current jumps to a high value and drops rapidly (not resolved because of the sample capacitance). It then decreases more slowly, reaching a minimum in the msec range and increases again until reaching stationarity after about 10 sec. With decreased light intensity, the time constant to achieve stationarity is increased and a second minimum appears in the low μsec range. Both minima shift to longer times with decreasing intensity (shown for the "slow" minimum in Fig. 9). The minima are more pronounced at lower temperatures [compare Figs. 8(a) and 8(b)]. The current ratio between stationarity and deepest minimum is almost one order of magnitude at 155 °K and about a factor of two at 220 °K. The time of the slow minimum increases with applied voltage as shown in Fig. 10. and is somewhat shorter at lower temperatures.

When biased in forward direction, however, the stationary current is essentially attained within a few microseconds with only a very small drift down of a few percent over 10 sec [Fig. 8(a)]. As expected, in the forward direction no cathode-adjacent high-field domains are observed. (Anode-adjacent domains[7] form at applied voltages considerably above the critical voltage at which cathode-adjacent domains are observed in reverse direction, and are not investigated here since they do not allow an unambiguous determination of the field at x_0.)

Because it is important to have information about the level distribution in the band gap where space charge can be stored for the following discussion, the current methods of thermally stimulated current (TSC)[11] and spectral distribution of the photocurrent (SDP)[12] were employed. Since it is observed that CdS platelets, doped by a procedure similar to that used for the investigated crystals, show very similar TSC and SDP behavior, the latter measurements were done with a different, but

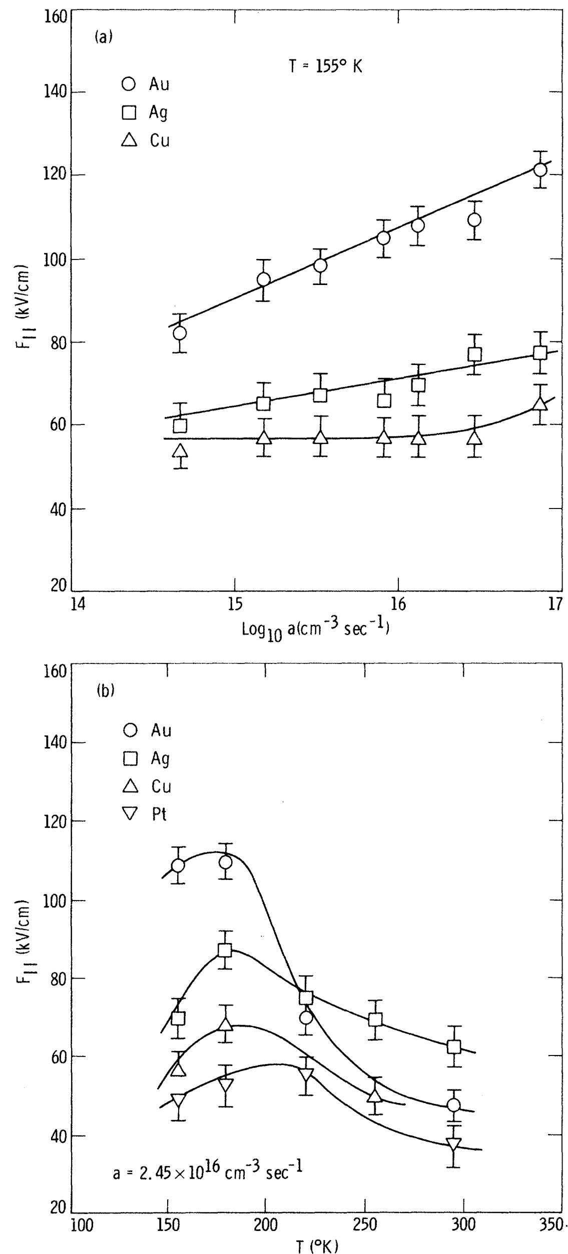

FIG. 6. Field F_{II} in the high-field domain as a function of optical excitation (a) and temperature (b).

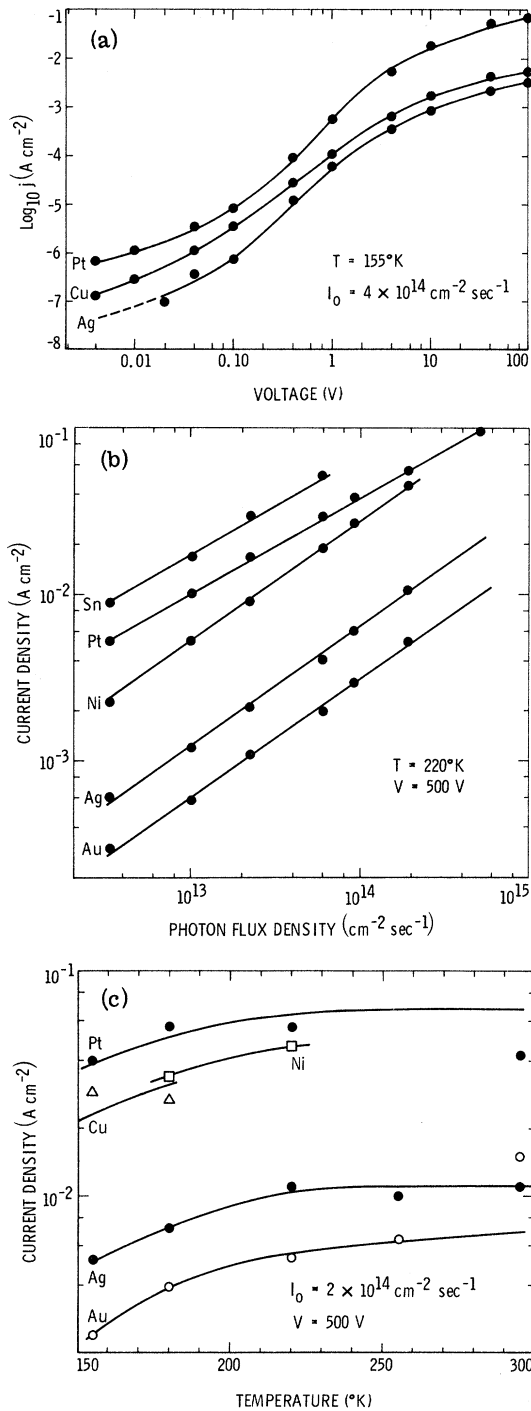

FIG. 7. Current density as a function of voltage (a), optical excitation (b), and temperature (c) for various cathode metals on photoconducting CdS.

similarly doped, CdS platelet. Figure 11 shows two TSC curves: (1) optical excitation (at the band edge) applied only at liquid-nitrogen temperature and (2) optical excitation applied during cooling (sliding wavelength with shifting band edge) starting at room temperature, so as to fill repulsive traps. Figure 12(a) shows the SDP for two different temperatures, and Fig. 12(b) shows the electron lifetimes as a function of temperature.

VI. DISCUSSION

A. Properties of the Homogeneous Crystal

Since crystals cleaved in vacuum behave in every investigated respect similarly to the ones prepared after exposure to air, we must assume that the defect-level density of the crystals extends homogeneously to the actual electode-CdS interface. Hence, a trap-level analysis using TSC curves gives useful information about the level density above the Fermi level in the entire CdS crystal (i.e., also in the range $0<x<x_0$).

We will, therefore, first study the trap distribution in order to aid later estimates on space-charge formation close to the electrodes. The trap density can be obtained from

$$N_t \simeq \frac{a}{i_0}\int_{t(T_1)}^{t(T_2)} i_{\mathrm{TSC}}\,dt \,, \tag{11}$$

where i_0 is the photocurrent at an optical excitation

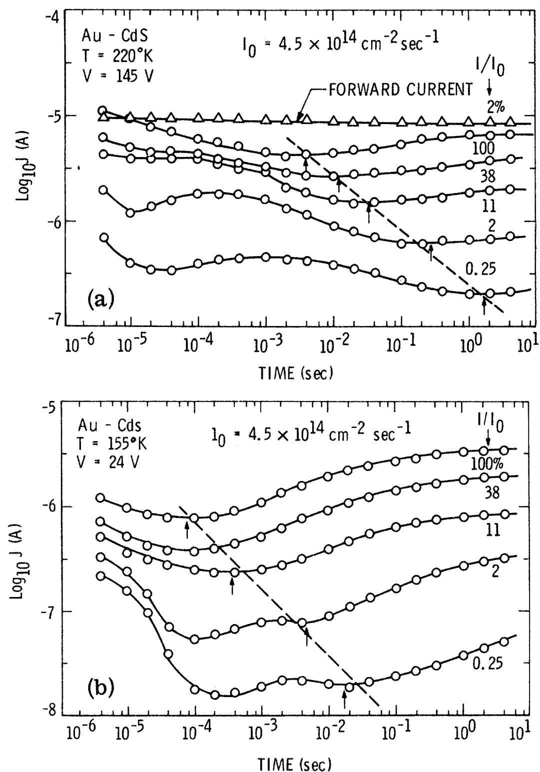

FIG. 8. Time-dependent current with optical excitation as a variable for a temperature of (a) 220 °K and (b) 155 °K.

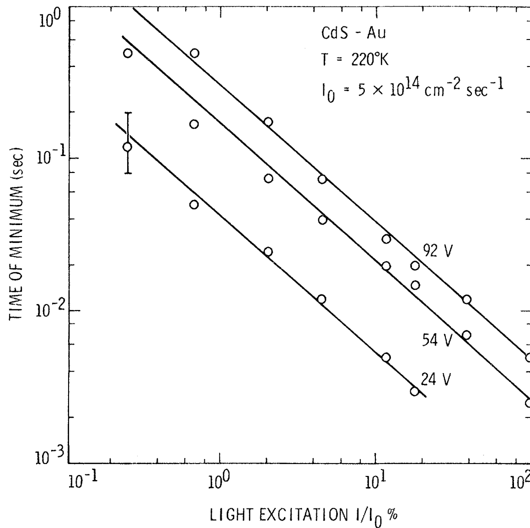

FIG. 9. The dependence of the "slow" minimum shown in Fig. 8(a) on light excitation with voltage as a variable.

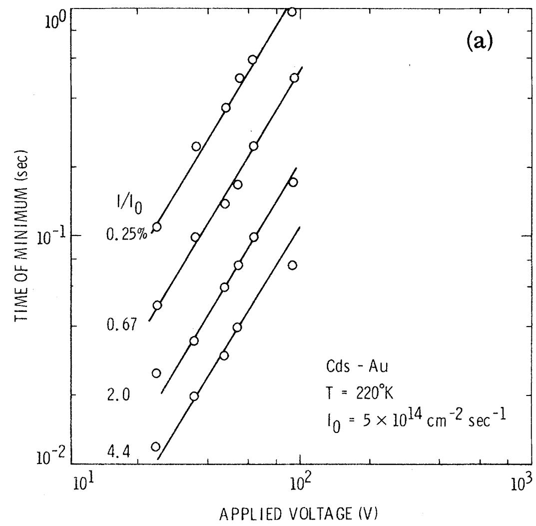

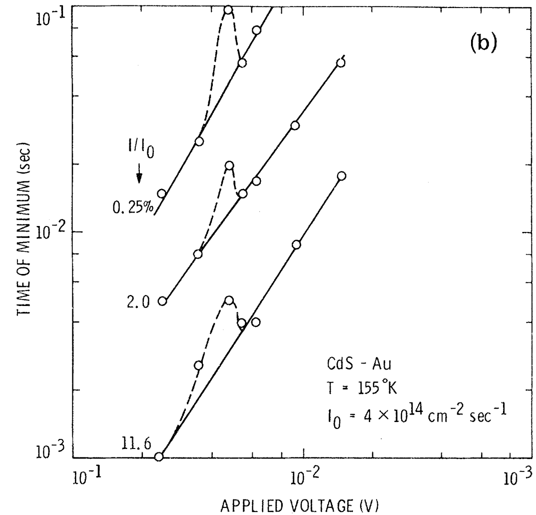

FIG. 10. The dependence of the "slow" minimum on applied voltage with light excitation as a variable for (a) $T = 200$ °K and (b) $T = 155$ °K.

density a and at the temperature of the TSC peak; T_1 and T_2 are the low- and high-temperature values of the $1/e$ points of the peak, respectively. The energy of the trap level $(E_c - E_t)$ related to the TSC peak may be estimated by

$$E_c - E_t \simeq kT_p \ln(N_c/n_p) \tag{12}$$

with T_p the temperature, and n_p the free-electron density at the TSC peak.

From Figs. 11 and 12 we obtain values of the trap density and energy for the different traps as given in Table I.

The trap densities are obviously too small (by at least two orders of magnitude) to accommodate a space-charge density necessary to change fields in the 10^5-V/cm range over distances of the order of the mean free path (see Sec. 2).

The spectral distribution of the photoconductance shows a typical class-II behavior[13] indicating essentially homogeneous doping[14] and volume photoconductivity, thereby allowing for determination of carrier densities n_i in the bulk of the CdS crystal from the measured current and the crystal dimensions. These carrier densities are typically in the 10^{12} cm^{-3} range for the unquenched case (100% optical excitation) and about two orders of magnitude smaller in the high-field domain. They are more than five orders of magnitude above n_b for $\psi \simeq 0.8$ eV and $T \leq 300$ °K, indicating blocking contact conditions. Such conditions $(n_b \ll n_i)$ are fulfilled for *all* investigated metal-CdS combinations $(0.5 < \psi < 0.8$ eV) for all investigated temperatures (155 °K < T < 300 °K).

TABLE I. Results from thermally-stimulated-current measurements.

Temperature of TSC peak (°K)	130	220	330
Energy of trap, $E_c - E_t$ (eV)	0.3	0.5	0.7
Density of trap $N_t(E_t)$ (cm^{-3})	7×10^{15}	7×10^{15}	2×10^{16}

B. Current-Voltage Characteristics

In this paper we are concerned only with reverse bias current in order to analyze the mechanism of carrier transport across the potential barrier of

a blocking contact.

The main current mechanisms for a photoconductor, as discussed in Sec. II are: (a) thermionic emission, (b) extraction of holes, and (c) tunneling.

Since the current in the case of the thermionic emission is limited by Eq. (3), the current cannot be supplied by this mechanism for higher voltages. At 300 °K the limiting currents are of the order of 10^{-8} A cm^{-2} for $\psi = 0.8$ eV and 3×10^{-5} A cm^{-2} for $\psi = 0.6$ eV. From Fig. 7 it can be seen that these limiting currents are already surpassed at voltages smaller than, or of the order of, one volt. At lower temperatures, since n_c decreases exponentially with T, the limits are even lower.

Extraction of holes can be an active mechanism only if the gain factor is small enough ($G \ll 1$). The gain factor ($G = j/eaL$), becomes of the order of one for values of j of the order of 10^{-4} A cm^{-2} for the higher photon flux. In Fig. 7 this situation is typically arrived at an applied voltage of one volt. For lower photon fluxes, the current decreases linearly or less than linearly with the light intensity, and therefore, the situation is arrived at the same or even lower voltages.

This allows us to separate the following ranges: (i) Low applied voltages: thermal emission (at high temperatures) and/or hole extraction (at low temperatures) predominates. (ii) High applied voltages: tunneling through the barrier predominates. The transition from range (i) to (ii) occurs at or below one volt for the crystals discussed here.

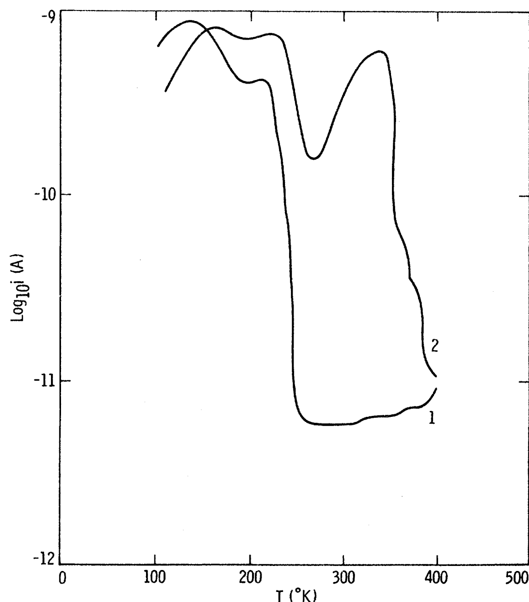

FIG. 11. Thermally stimulated current with band edge optical excitation applied only at (1) 80 °K and (2) applied during cooling so as to fill repulsive traps.

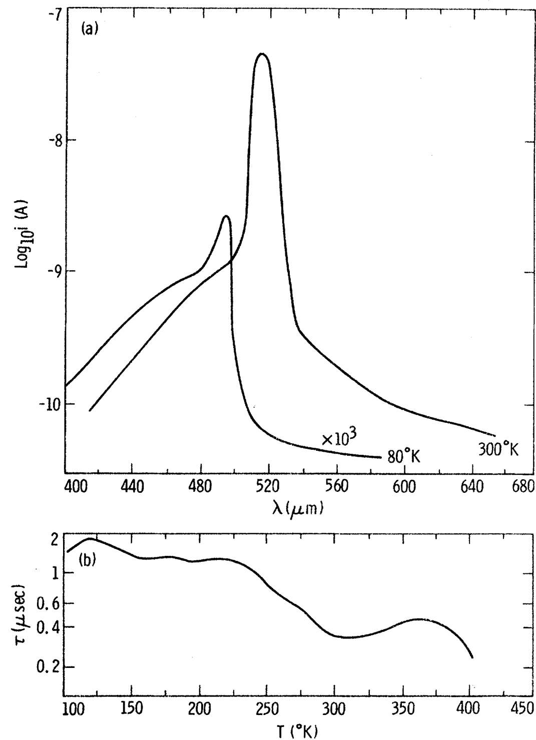

FIG. 12. (a) Spectral distribution of the photoconductance for two different temperatures and (b) the electron lifetimes for the bulk computed from such curves as a function of temperature.

Our major discussion will deal with range (ii) in which tunneling predominates. Current densities above 10^{-4} A/cm^2 obviously require fields of the order of 10^6 V/cm at the barrier with the top of the barrier well within 100 Å from the electrode interface.[2] Hence, x_0 is much larger than x_b, and we must conclude that a high density space-charge layer is formed in the region $0 < x < x_0$. With x_0 of the order of 10^{-5} cm, as shown in the following paper,[3] this positive space-charge layer must have a density of at least 10^{18} cm^{-3} [Eq. (7)] in order to reduce the field at x_m from 10^6 V/cm, necessary for tunneling, to a value which is at least one order of magnitude lower at x_0. The maximum value of the field at x_0 is unambiguously given as the field in the high-field domain.

The high space-charge density required for tunneling which cannot be accommodated in the known part of the level distribution of CdS prompted us in an earlier publication[1] to reject tunneling, and to suggest a lowering of the work function caused by the flux of holes into the barrier region as the determining mechanism. A more detailed analysis[3] of the barrier properties, however, renders such an explanation improbable. Hence, there seems to be only one possibility left for the currently known

mechanism, namely, to assume that in photoconducting CdS a sufficient density of levels exist in an energy range currently inaccessible for defect-state analysis, i.e., near the (dark) Fermi level (about 0.8 eV below the conduction band). Such levels must be produced by native defects since the density of impurities is well below 10^{18} cm^{-3}. These native defects may be the reason why bulk CdS cannot be made p-type via diffusion doping.

If tunneling or multiple-step tunneling is indeed the predominant mechanism for the carrier transport at high current densities, one must then explain why different contact metals cause a marked shift in the current-voltage characteristics and cause different singular points II well separated from the minimum current quasisingular point II* (see Figs. 2 and 3).

Since different metal-CdS combinations result in different barrier heights, one would indeed expect different tunneling probabilities, hence different currents, as long as the tunneling markedly limits the current. Such a limiting effect may disappear only for very thin barriers caused by excessive space-charge densities. Then, the individuality of the metal is expected to vanish with respect to its influence on the characteristics, as observed for contacts evaporated onto CdS after the near-surface region is highly disordered by means of a gas discharge.[15]

A pronounced influence of the metal on the singular points is expected as long as the carrier density at x_0 is above the minimum carrier density for the fully quenched case (at II* in Fig. 3). This can be seen by following the field and carrier density from x_m to x_0 (Fig. 1). As $F(x)$ decreases, $n(x)$ increases with a slope controlled by the space-charge density. For a higher barrier, $F(x_m)$ must be larger to provide the same current; hence, $F_{II} \simeq F(x_0)$ must be larger if x_0 and ρ are independent of F. Although the latter is not the case, it is highly improbable that changes in x_0 and ρ due to the field compensate exactly for changes in $F(x_m)$. Hence, F_{II} should depend on the electrode material, as observed. However, if the defect density is small enough so as to increase the carrier density at x_0 to a value not exceeding the minimum density $n(\text{II}^*)$ [or not to decrease the field at x_0 below $F(\text{II}^*)$], the individuality of the metal should be unobservable in the high-field domain regime. We will return in more detail to this discussion in the following paper.[3]

The distinct difference between materials showing different current behavior for different "blocking" contacts and materials not showing such differences can, therefore, be attributed to the density of levels which can cause a positive space charge in a slab of thickness x_0. Because of nearly perfect charge compensation of defects with such density in the bulk, a positive space charge can be produced by lifting this compensation via excitation of electrons from deep donors (0.8 eV below E_c) and extracting these electrons from the barrier region. Such excitation is easily possible via multiple-step tunneling[2] of field-enhanced ionization.[16]

Regarding the time dependence of the current, it is important to note the two minima that appear in the transient. A decrease in current as time increases involves a redistribution of the electric field, which decreases in the bulk, and consequently (due to the constancy of the total applied voltage) increases in the contact region. An undershoot of the current (the fact that it takes values below its final equilibrium value) indicates that a current source is being exhausted. The fact that there are two minima therefore suggests that there are at least two different sources of current generation which are exhausted at different times and finally replaced by tunneling.

In the following paper[3] we will analyze the barrier region in more detail and substantiate the assumptions made in this paper. We will also discuss the transient behavior of the current, which depends strongly on the properties of the barrier region.

ACKNOWLEDGMENTS

The authors wish to express their appreciation to L. van den Berg for growing and to J. Phillips and H. Hadley for doping of the CdS crystals, and to W. A. Hermann for his careful work in preparing the samples. The measurement of $n_1(F)$ by J. Phillips is gratefully acknowledged.

*This paper presents the results of one phase of research sponsored by the National Aeronautics and Space Administration under Contract No. NAS 7-100 and the U. S. Office of Naval Research, Washington, D. C.

†Present address: Comisión Nacional de Energie Atómica, Buenos Aires, Argentina.

[1]R. Stirn, K. W. Böer, G. A. Dussel, and P. Voss, in *Proceedings of the Third International Conference on Photoconductivity*, edited by E. M. Pell (Pergamon, Oxford, 1971), p. 389.

[2]G. H. Parker and C. A. Mead, Appl. Phys. Lett. **14**, 21 (1969).

[3]G. A. Dussel, K. W. Böer, and R. J. Stirn, following paper, Phys. Rev. B 7, 1443 (1973).

[4]K. W. Böer and P. Voss, Phys. Rev. **171**, 899 (1968).

[5]K. W. Böer, G. Dohler, G. A. Dussel, and P. Voss, Phys. Rev. **169**, 700 (1968).

[6]G. A. Dussel and K. W. Böer, Phys. Status Solidi **39**, 391 (1970).

[7]K. W. Böer and P. Voss, Phys. Status Solidi **28**, 355 (1968).

[8]K. W. Böer and K. Bogus, Phys. Status Solidi **176**, 899 (1968).

[9]B. K. Ridley, Proc. Phys. Soc. Lond. **82**, 954 (1963).

[10]The density of dopants was chosen so as to achieve a steep transition between the high field in the domain and the low field in the adjacent crystal, hence, an unambiguous detection of the domain boundary.

[11]G. A. Dussel and R. H. Bube, Phys. Rev. **155**, 764 (1967).

[12]R. H. Bube, *Photoconductivity of Solids* (Wiley, New York, 1960).

[13]R. Schubert and K. W. Böer, J. Phys. Chem. Solids **32**, 71 (1971).

[14]Homogeneous doping is also indicated from the observed linear dependence of the width of a high-field domain on the applied voltage.

[15]J. Fassbender, Z. Phys. **145**, 310 (1953).

[16]G. A. Dussel and K. W. Böer, Phys. Status Solidi **39**, 375 (1970).

PHYSICAL REVIEW B VOLUME 7, NUMBER 4 15 FEBRUARY 1973

Photoconductor-Metal Contact at Higher Densities*

G. A. Dussel† and K. W. Böer
Department of Physics, University of Delaware, Newark, Delaware 19711

R. J. Stirn
Jet Propulsion Laboratory, Pasadena, California 91103

(Received 9 June 1971)

The formation of space charge in the barrier region is discussed. This region extends to $x_0 \simeq 200$ Å $+2\lambda$ (λ is the mean free path of majority carriers). The conventional transport equation can be used only for $x > x_0$, and the carrier density at x_0 represents a boundary condition for the bulk. Its change as a function of applied voltage, temperature, and light intensity in photoconducting CdS is discussed. The time dependence of the space-charge formation in the region $0 < x < x_0$ is analyzed. It is shown under which conditions the individuality of the metal contact is observable.

I. INTRODUCTION

In the preceding paper[1] we have shown that at higher current densities, a model using a simple carrier transport and Poisson equation to explain the behavior in the barrier near a "blocking" cathode breaks down. This situation can be reached with photoconducting CdS and with current densities greater than $\sim 10^{-7}$ A/cm^2. It was suggested[1] that tunneling through the barrier is the major effect to provide current continuity. This is in agreement with the suggestions made earlier by several authors (for a summary, see Ref. 2) and by itself does not seem to necessitate a careful new study. However, the recently developed method of high-field domains[3] made it possible to determine unambiguously the maximum field F_{II} starting at a distance x_0 from the electrode interface. The distance x_0 is that distance from the interface beyond which the simple transport equation

$$j = e\mu(F)\, n(F)\, F - \mu k T \frac{dn}{dx} \quad , \tag{1}$$

and Poisson equation

$$\frac{dF}{dx} = \frac{e}{\epsilon\epsilon_0}\,\rho(n, F) \tag{2}$$

are valid. This maximum field F_{II} is too low and x_0 is too small to accommodate enough space charge in a slab $0 < x < x_0$ in lightly doped photoconductors ($N_D < 10^{17}$ cm^{-3}) to reach critical fields necessary for sufficient tunneling. We therefore had to assume that additional donors of $\sim 10^{18}$ cm^{-3} are always present in CdS at an energy not accessible to conventional detection methods, since no other known process but tunneling could account for the observed current densities. We have investigated[1] the stationary and kinetic behavior of the current across a barrier caused by different metal-CdS combinations, and in this paper will give a more detailed analysis of the process taking place in the thin (of the order of a few mean free paths of majority carriers) barrier layer ($0 < x < x_0$).

II. IMAGE FORCE REGION

The potential distribution in the barrier region is determined by four factors: (i) the image forces, (ii) the difference of work functions between the metal and the photoconductor, (iii) the space-charge distribution determined by the carrier kinetics, and (iv) the external field. The image force of a carrier is attractive toward the metal and its potential is given by

$$V(x) = \frac{e}{16\,\pi\epsilon_0\epsilon_\infty x} \quad , \tag{3}$$

where ϵ_∞ is the optical dielectric constant and ϵ_0 is the permittivity of free space. This potential distribution is shown in Fig. 1 for electrons and holes. It should be pointed out that close to the photoconductor-metal interface there is no change in the band gap, as it appears from Fig. 1, because an image force is experienced by either an electron (both bands bend downward) or by a hole (both bands bend upward) if they are located close to the electrode. However, when an electron and a hole are closer together than their separation from the electrode, a dipole-dipole interaction re-